Characteristics of one-year observational data of VOCs, NO_x and O_3 at a suburban site in Guangzhou, China

Y. Zou[1,2], X. J. Deng[1,2], D. Zhu[2], D. C. Gong[2], H. Wang[3], F. Li[1], H. B. Tan[1], T. Deng[1], B. R. Mai[1], X. T. Liu[1], and B. G. Wang[2]

[1]Institute of Tropical and Marine Meteorology/Guangdong Provincial Key Laboratory of Regional Numerical Weather Prediction, CMA, Guangzhou, China

[2]Institute of Atmospheric Environmental Safety and Pollution Control, Jinan University, Guangzhou, China

[3]Department of Applied Physics, University of Eastern Finland, Kuopio, Finland

Received: 3 June 2014 – Accepted: 21 June 2014 – Published:

Correspondence to: X. J. Deng (dxj@grmc.gov.cn) and B. G. Wang (tbongue@jnu.edu.cn)

Published by Copernicus Publications on behalf of the European Geosciences Union.

Abstract

Guangzhou, one of megacities in China, is beset with frequent occurrence of high-concentration ozone events. In this study, online instruments were used to simultaneously monitor ozone, nitrogen oxides (NO_x) and volatile organic compounds (VOCs) at GPACS (the Guangzhou Panyu Atmospheric Composition Station) of the China Meteorological Administration, from June 2011 to May 2012, in order to determine their characteristics, the effect of VOCs on ozone photochemical production and the relationship between VOC/NO_x ratio and ozone formation. The results showed that during the observation period, seasonal variation of ozone concentration was lower in spring and winter, compared to summer and autumn, which is contrary to that for VOCs and NO_x. In terms of VOCs, aromatics had the largest ozone formation potential, among which toluene, xylenes, ethylbenzene, 1,2,4-trimethylbenzene and 1,3,5-trimethylbenzene were the most important species, with a total contribution of about 44%. As the VOC/NO_x ratios were very high during high-concentration ozone events that occur all year round, we speculate ozone production was likely to be NO_x-limited regime (12:00-16:00LT) in Guangzhou. Further investigations based on numerical models are needed in the future, to obtain more detailed and robust conclusions.

1 Introduction

Along with its rapid economic development and urbanization, the Pearl River Delta (PRD), whose major cities include but not limited to Hong Kong, Guangzhou, Dongguan and Shenzhen, has become one of the most polluted areas in China (Chan et al., 2008). Unlike other regions in China, such as the surrounding Beijing region and the Yangtze River Delta region, where the main air pollutant is particulate matter (Wang et al., 2012; Zhao et al., 2011), high-concentration ozone events occur frequently in the PRD (Wang et al., 2009), due to its unique geographical location and climate, as well as a rapid increase in the emission of ozone precursors (VOCs and NO_x) from industrial activities and motor vehicles.

Tropospheric ozone is the secondary pollutant generated by the photochemical reaction of VOCs and NO_x in the presence of sunlight (Sillman, 1995). Smog chamber studies have been widely used to investigate the gas-phase photochemical transformations of NO_x and VOCs, as well as their roles in ozone production. It has been found that VOCs and NO_x have no linear relationship with ozone formation. Instead, their impact on ozone formation can be described by VOC- or NO_x-limited regimes (Zhang et al., 2004; Tie et al., 2007; Geng et al., 2008). Numerical simulations in polluted regions, such as Los Angeles in the 1980s, have shown ozone formation to be NO_x-limited when the VOC/NO_x ratio is greater than 8:1, for VOC expressed as concentration of carbon atom (Seinfeld, 1989), a finding which many researchers later used to explain photochemical ozone formation in other areas, where specific atmospheric situations may differ (Trainer, 1993; Sillman, 1999; Seinfeld, 1991; Ran et al., 2009, 2011; Li et al., 2008). Also, there is increasing evidence to show that ozone formation may change with the time of day (Li et al., 2013; Kanaya et al., 2009; Sillman and West, 2009). For example, a recent study reported that ozone formation was VOC-limited in the morning and became NO_x-limited during peak ozone hours in most of the PRD region (Li et al., 2013). Such temporal variations in ozone formation have also been documented for other places in the world (Kanaya et al., 2009; Sillman and West, 2009).

In order to understand and therefore reduce the formation of ozone, it is critical to evaluate the relative importance of various VOCs in terms of ozone production potential, because individual VOCs exhibit a wide range of reactivity with respect to ozone photochemical formation. Several reactivity scales have been used to assess the relative ozone forming capacity of individual VOCs species (Atkinson, 1990; Carter, 1994; Li and Wang, 2012; Shao et al., 2009). One widely used scaling method is the Maximum Incremental Reactivity (MIR), defined as the maximum amount of ozone formed per unit of VOCs added or subtracted from the whole gaseous mixture in a given air mass, which considers the chemical mechanism and the impact of VOC/NO_x ratio on ozone production (Atkinson, 2000). Another common approach is the OH-reactivity scale (e.g. propylene-equivalent concentration), which is based on assumptions that the reactions with OH radicals are dominant in the tropospheric atmosphere and that the mechanistic factor and its associated uncertainties are negligible (Derwent et al., 1976; Middleton et al., 1990).

The formation and levels of ozone pollution have been investigated in many megacities around the world (Qin et al., 2004; Stephens et al., 2008) and a number of studies have also been conducted to explore the formation of ozone in the PRD (Wang et al., 2005; Cheng et al., 2010; Guo et al., 2009). Most of these studies have shown that ozone formation was

VOC-limited in the PRD region (Zhang et al., 2008b; Guo et al., 2009). However, little long-term observational data are available for ozone, NO_x and VOCs in the PRD, in particular, continuous VOC data (Wang et al., 2004; Shao et al., 2009), which only serves to limit our understanding of ozone production.

This study aimed to explore the characteristics of VOCs, NO_x and ozone, and to examine the possible seasonal and diurnal variations in ozone formation in the PRD based on one-year of observational data for ozone and its precursors collected in Guangzhou, one of megacities in PRD. In the present paper, we document general information about the sampling site and the data collection procedure (Sect. 2), as well as the seasonal and diurnal characteristics of ozone and its precursors (Sect. 3.1). The effects of VOCs on ozone formation, based on estimated MIRs and propylene-equivalent concentrations, are also presented (Sect. 3.2) and finally, ozone formation regimes in Guangzhou are discussed, based on variations in VOC/NO_x ratios (Sect. 3.3).

2 Experimental

2.1 Site description

From June 2011 to May 2012, Simultaneous measurements of ozone, NO_x and VOCs by online instruments were carried out at the Guangzhou Panyu Atmospheric Composition Station (GPACS) of the China Meteorological Administration. The GPACS site (23°00'N, 113°21'E, 141 m a.s.l.) is located on the mountain top of Dazhengang, Nancun Town, Panyu District, Guangzhou, China (Fig. 1). It is a suburban site (about 15 km southwest of downtown Guangzhou) where high-concentration ozone events often occur, and it is also one of the main observation sites for atmospheric composition in the PRD. As seen in Fig. 2, regardless of the large variation in concentration of the three categories of VOCs (i.e. alkanes, alkenes and aromatics), their relative contributions remained fairly uniform throughout the observational period. Such uniformity implies that the air at the GPACS site was sufficiently homogenized from various sources near the surface of the ground. The prevailing wind, wind speed and temperature at the sampling site during different seasons are shown in Fig. 3 and Table 1. At the sampling point, northeasterly and southwesterly winds prevailed in spring (March, April, and May), along with southwesterly winds in summer (June, July and August), southwesterly winds in autumn (September, October and November) and northeasterly winds in winter (December, January and February). During the different seasons, the average wind speed remained close to 1.4 $m.s^{-1}$, while the average temperature ranged from 14.2 ^oC in winter to 29.4 ^oC in summer. When the prevailing wind was northeasterly in December, the difference between weekend and weekday VOC concentration was very clear, indicating that large amounts of pollutants were emitted from downtown Guangzhou City. When the prevailing wind was southwesterly in July, the difference between weekend and weekday VOC concentration was mild, indicating that only small amounts of pollutants were emitted from the outer suburban areas.

2.2 Instrument description

Ozone was measured using an EC9810B ozone analyzer (Ecotech Co., Australia) based on the UV-absorption method and the Lambert-Beer Law. NO_x was measured by an EC9841B nitrogen oxide analyzer (Ecotech Co., Australia) with a heated molybdenum NO_2 to NO converter and gas phase chemiluminescence technology was used to quantify NO concentrations. It was possible that the measured NO_x may have included some oxidized reactive nitrogen that was converted by the molybdenum, and thus, the NO_x concentrations given below are considered the upper limits of their actual values (Dunlea et al., 2007, Ran et al., 2011).

VOCs were continuously monitored at a 1-hour sampling frequency using the GC5000 analysis systems coupled with flame ionization detectors (FID) from AMA Instruments GmbH (AMA, Germany). This system has been described in detail elsewhere (An et al., 2014; Zou et al., 2013). In brief, it consisted of two sets of sampling systems and two sets of chromatography column systems, which includes a low boiling point VOC analyzer (GC5000VOC) for C_2-C_6 VOC species and a high boiling point VOC analyzer (GC5000BTX) for C_6-C_{12} VOC species. Air samples were enriched in the GC5000VOC analyzer through two-stage trap, and then thermally desorbed when the temperature increased to 200 ^oC, followed by separation with two-dimensional chromatography. The chromatographic columns consisted of an Al_2O_3/Na_2SO_4 plot column (60 m × 0.32 mm inner diameter × 5 μm thickness) and a CARBOWAX^{TM} back flushing column (30 m × 0.32 mm inner diameter × 0.25 μm thickness). The back flushing column was firstly used to remove the moisture component and high-boiling VOC species, and then the plot column was followed to separate the low-boiling VOC species. The GC5000BTX pre-concentrated the VOCs at 30 ^oC and then thermally desorbed them at 270 ^oC; afterwards, the analyzer separated the compounds in the DB-1 column (60 m × 0.32 mm inner diameter × 10 μm thickness), in order to achieve optimum separation and prevent interference from related compounds.

The 56 VOCs designated as photochemical precursors by the United States Environment Protection Agency were used as the target compounds. The gas standard used was the same as that used by the EPA/USA Photochemical Assessment Monitoring Stations (PAMs). Zero and span gas checks (using PAM calibration gases) were conducted monthly throughout the observation period, together with adjustment of the retention time. Five-level calibration curves were used to quantify the VOC concentrations during the online monitoring. The calibration curves and detection limits of individual VOCs are listed in Table 2. The correlation coefficient ranged from 0.984 to 0.999, and the detection limits ranged from 0.03 ppbv to 0.09 ppbv. Outliers were eliminated before data processing, to guarantee the validity of the data. However, the instruments were not intercompared with other VOC measurement systems, and that such an intercomparison is an important priority for future work.

3 Results and discussion

3.1 Characteristics of ozone, NO_x and VOCs

The seasonal and diurnal variation characteristics of ozone, VOCs and NO_x are shown in Fig. 4. The seasonal variation of ozone is readily apparent, being lower in the spring and winter, and higher in the summer and autumn. Furthermore, the range of increase is much larger in

late spring and early summer than the other periods, which is mainly due to the sunlight, ambient temperature, other meteorological factors and emission strength of air pollutants being different during each season (Bloomer et al., 2009, 2010). In contrast, seasonal variation in the concentration of ozone precursors was opposite to that of ozone concentration, with NO_x concentration being higher in spring and winter and VOC concentrations higher in winter compared to summer. Average concentrations of VOCs, NO_x and ozone in each season are shown in Table 3. The average concentration of VOCs was about 42.74 ppbv, varing from 34.60 ppbv in March to 63.57 ppbv in November, while the average concentration of NO_x was about 35.51ppbv, ranging from 21.75 ppbv in August to 76.39 in March, and ozone concentration varied from 9.31 ppbv in January to 29.67 ppbv in September. The diurnal variation of ozone concentration was unimodal, reaching its maximum at 14:00 LT, while the ozone precursors (VOCs and NO_x) showed bimodal variation, with a peak during rush hours, although these variations were not always apparent for some seasons. These variations in diurnal concentration indicate that photochemical precursors gradually decreased, while their products increased. It should be noted that the measured NO_x concentrations are in fact upper limits, because the NO_x probably includes some oxidized reactive nitrogen that was is converted by the molybdenum. In order to further understand the variation in ozone concentration and reveal its dependence on photochemical reactions, it is necessary to analyze the change rates of ozone, with respect to time, in each season, shown as follows:

$$\frac{d[O_3]}{dt} = [O_3]_{t+1} - [O_3]_t \quad (1)$$

In the equation, $[O_3]_t$ represents the ozone concentration at time *t*, and $[O_3]_{t+1}$ is the ozone concentration for the next hour after time *t*. In the absence of transport effects, a negative change rate in ozone concentration indicates that the chemical loss of ozone plays a dominant role in the variation of ozone concentration, while the contrary indicates the fact that the generation of ozone photochemical reactions plays a key role. Although wind speed is low at this site, the effect of horizontal transport on daily variation in ozone concentration is difficult to estimate and cannot be ruled out. Here, we interpret all variations as due to chemical production and loss, understanding that such interpretation is an upper limit to the effect of chemistry, due to the likelihood of transport also influencing daily ozone variation. Although diurnal variations in the change rate of ozone for different seasons show little difference, the results indicate that a negative change rate in ozone concentration occurs at about 15:00 LT. At this time, there was a decrease in OH radicals due to the fact that sunlight, and its associated photochemistry, begins to decrease. At about 19:00 LT, there were no OH radicals present, however the titration of ozone by emissions of NO_x could still consume ozone, and it was not until 0:00-7:00 LT that the ozone concentration was seen to stabilize. After this, the concentration of ozone began to show a positive change at 8:00LT, due to the breakup of the nocturnal boundary layer and increased photochemistry (Fig. 5).

3.2 The effect of VOCs on ozone formation

VOCs exhibit a wide range of reactivity, and their concentrations are not proportional to ozone photochemical formation. The average concentration of VOCs (ppbv) in each season has been discussed in Sect. 3.1. In order to adequately understand the properties of VOCs

observed in the ambient atmosphere and to identify their critical role in ozone photochemical production, VOC composition and reactivity have long been of particular concern. VOCs have two main characteristics that determine their ozone formation potential: kinetic reactivity and mechanism reactivity. To estimate the reactivity of VOCs according to their kinetic reactivity, we calculated the Propy-Equiv concentration (Chameides et al., 1992; Lawrimore et al., 1995):

$$C_{j,Propy-Equiv} = C_{j,C} \times \frac{K_{j,OH}}{K_{Propy,OH}} \quad (2)$$

where j represents a species of VOC, $C_{j,C}$ represents the carbon atom concentration (ppbC) of this species, and $K_{j,OH}$ and $K_{Propy,OH}$ denote the chemical reaction rate constant in the free radical reaction of species j and propylene with OH. $K_{j,OH}$ is obtained from studies by Atkinson and Aery (Atkinson and Aery, 2003). To estimate for the reactivity of VOCs by the mechanism reactivity, the MIR-weighted concentration, which represents the maximum ozone concentration generated by this species based on estimated MIR, was calculated as per the equation below:

$$C_{j,MIR} = MIR_j \times C_{j,ppbv} \times \frac{m_j}{M} \quad (3)$$

where $C_{j,ppbv}$ represents the actual concentration by volume (ppbv) for species j, M represents the molecular mass of ozone, and m_j represents the relative molecular mass of species j in the VOCs. The MIR_j was estimated by selecting the specific MIR value for each of the VOCs from published studies which were conducted based on modelled scenarios for Los Angeles in the 1980s (Carter et al., 1994; Dodge, 1984). The OH reaction rate constants and estimated MIR coefficients, as well as their concentrations, for each VOC species are shown in Table 4.

Fig. 6 shows the characteristics of each VOC category obtained at the sampling point, with concentrations expressed by different scales. As can be seen from the non-weighted concentration by volume and by carbon atom, alkanes occupied the largest proportion, accounting for 59% and 53% of the VOC concentration, respectively, followed by aromatics (24% and 36%, respectively) and lastly alkenes (17% and 11%, respectively). As can be seen from the Propy-Equiv and MIR-weighted concentrations, the alkenes and aromatics were dominant, accounting for 73% and 83%, respectively. Total Propy-Equiv concentration accounted for nearly half of the carbon atom concentration, indicating that the reactivity of major VOCs species was lower than propylene at the sampling point. In summary, during the monitoring period, alkanes and aromatics were shown to have the highest concentration based on the concentrations by volume and carbon atom. However, based on ozone formation potential, aromatics and alkenes were found to make the largest contributions. While the alkane content was high, because of their low reactivity, they contribute less to the reactivity of VOCs and ozone formation potential. Although alkene concentrations were smaller than those of alkanes, due to their high reactivity, alkenes made a greater contribution to ozone than alkanes, which is consistent with findings from other locations (Russell, 1995).

Table 5 shows the ranking of ozone formation potential of VOC species, as calculated by the Propy-Equiv concentration and MIR factor methods, which both yielded similar results. Among the top ten species, eight species were the same, differing only in terms of rank order. As a result, both methods can be used to reflect the ozone formation potential of each VOC species, to some extent, especially for those which make a greater contribution to ozone

formation. However, since these two methods differ in principle, the calculated ranks of ozone formation potential are also different. The Propy-Equiv concentration method only considers kinetic activity and ignores the different mechanism activities of the reaction between peroxide radicals and NO, thus when assessing ozone formation potential, the species with a faster OH reaction rate, such as isoprene, may be overestimated. Although the MIR factor method considers the kinetics and mechanism activity, the MIR factor method is not a reliable approach for assessing ozone formation potential, due to the fact that the MIR factor involves possible uncertainty, as well as the lack of MIR data for some species (e.g. 1-hexene). In addition, it should be note that the MIR determined in one location may be different in another, such that the application of MIR may not be accurate in Guangzhou. In summary, aromatics were found to be the species with the highest reactivity at the sampling site, among which toluene, m-xylene, p-xylene, o-xylene, ethylbenzene, 1,2,4-trimethylbenzene and 1,3,5-trimethylbenzene made a total contribution of approximately 44% to ozone formation potential, followed by alkenes. Toluene, m-xylene, p-xylene and 1,3,5-trimethylbenzene are mainly sourced from large factories and industrial activities (Liu et al., 2008). Located in the eastern part of the sampling site, the industrial city of Dongguan (circle on the map in Fig. 1) are presumed to have made some contribution to these species at the sampling site in the autumn and winter, when northeasterly winds prevailed at the sampling site. Moreover, while isoprene concentrations were relatively low, it ranks at first and third in terms of OH reactivity and MIR, respectively. Therefore, isoprene emissions also need to be considered with respect to the control of ozone in Guangzhou.

3.3 Relationship between the variation of VOC/NO_x ratios and ozone formation regime

The impact of ozone precursors on ozone formation can be described as either VOC- or NO_x-limited. Assessing whether an area is VOC- or NO_x-limited is an important step towards reducing regional ozone pollution. The ratios of VOC/NO_x have been widely used to help determine the ozone formation regime. For example, numerical simulations of ozone pollution in Los Angeles in the 1980's indicated a transition from VOC-limited to NO_x-limited regime at a VOC/NO_x ratio of approximately 8:1 (Seinfeld, 1989). In this study, we did not perform any modeling work, but used the approximate VOC/NO_x ratio to determine if ozone formation was VOC- or NO_x-limited in Guangzhou. It is important to note that the actual VOC/NO_x ratio may be higher than the ratios reported here, as the measured NO_x may include some oxidized reactive nitrogen, due to the application of a molybdenum converter during the measurement phase.

Fig. 7 shows the diurnal variations of VOC/NO_x ratios, as well as ozone concentrations for each season during the measurement period. It can be seen that, in the summer and autumn, the average VOC/NO_x ratio was about 7:1 from 06:00-09:00 LT, and much higher than the 8:1 threshold for NO_x-limited formation from 12:00-16:00 LT, when ozone concentration reached a relatively high level. This indicates that ozone formation was likely to be VOC-limited during the morning and NO_x-limited during peak ozone hours, respectively. However, in the spring and winter, VOC/NO_x ratios were much lower than the ratio of 8:1, with an average value of about 7:1 and 5:1, respectively. The results suggest that ozone formation was more likely to be VOC-limited during the spring and winter.

Fig. 8 presents the frequency distributions of hourly ozone concentration for each season. As seen in the figure, high hourly ozone concentrations (i.e. ＞80 ppbv) were observed more frequently in summer and autumn, accounting for about 5% and 3%, respectively, followed by 2% in spring. Hourly ozone concentration did not exceed ＞80 ppbv in winter. As a result, ozone formation was more likely to be NO_x-limited during high-concentration ozone episodes in the PRD, a finding which is similar to that reported by Li et al. (2013). Considering that the impact of VOCs on ozone formation was more closely related to the reactivity of individual VOC species than to the amount of total VOCs, a VOC (reactivity)/NO_x ratio was used to analyze ozone formation (Fig. 7). The reactivity based VOC/NO_x ratio was consistent with the non-reactivity based VOC/NO_x ratio, due to the fact that, regardless of large variations in the concentration of the different types of VOCs (i.e. alkanes, alkenes and aromatics), the relative contribution of each type remained fairly uniform throughout the observation period, as it has been shown in Fig. 2.

Given that high-concentration ozone is particularly harmful to human health, many regulators are focusing on reducing emissions during peak ozone hours (12:00-16:00 LT) (Castellanos et al., 2009). In order to further study the relationship between the variation of VOC/NO_x ratios and ozone formation during high-concentration ozone events, 36 days with an hourly ozone value higher than 93 ppbv (i.e. 200 $\mu g.m^{-3}$), a threshold set by a new Chinese ambient air quality standard (GB 3095-2012) were selected for analysis during the monitoring period. Fig. 9 shows that the VOC/NO_x ratio during peak ozone hours (12:00-16:00 LT) was twice as high as the average ratio of 8:1 for summer and autumn, suggesting that ozone formation was likely to be NO_x-limited during peak ozone hours (12:00-16:00 LT) in Guangzhou. However, when ozone concentration was relatively low in the morning (6:00-9:00 LT) and at night (20:00-0:00 LT), the ratio of VOC/NO_x was about 6:1 and 7:1, respectively, which indicates that ozone formation was VOC-limited. It should be noted that, since we used the VOC/NO_x ratio of 8:1 from Los Angeles to determine ozone formation regimes in Guangzhou, no definitive conclusions can be drawn, in terms of limiting NO_x or VOCs to control ozone formation, in the absence of a photochemical model, together with more accurate measurements of NO_x in the Guangzhou region.

4 Conclusions

Ground-level ozone and its precursors (i.e. VOCs and NO_x) were monitored over a 12 month period (from June 2011 to May 2012) at GPACS, which is located in a suburban area of Guangzhou, where high ozone events often occur. Observation-based analysis was performed to investigate the characteristics of VOCs, NO_x and ozone in this highly populated region.

Ozone concentration was significantly higher in summer and autumn, while the opposite was observed for VOCs and NO_x, which were higher in winter and spring. Ozone concentration began to show a net increase at 8:00 LT, likely due to the breakup of the nocturnal boundary layer and increased photochemistry, while a net decrease in ozone concentration occurred at about 15:00 LT, due to the fact that sunlight, and its associated photochemistry, begin to decrease, leading to low OH radicals and the titration of ozone by emissions of NO_x. In terms of reactivity-based concentration of VOCs, aromatics had the largest ozone formation potential, among which toluene, m-, o- and p-xylene, ethylbenzene,

1,2,4-trimethylbenzene and 1,3,5-trimethylbenzene made a total contribution of approximately 44% to ozone formation potential. It should be noted that while the concentration of isoprene emitted by plants is not high, it makes a large contribution to ozone formation (about 8%), due to its high MIR reactivity.

We also examined the temporal characteristics of ozone formation regimes according to the ratio of VOC/NO_x, which indicated that ozone formation was likely to be NO_x-limited during peak ozone hours (12:00-16:00 LT) in summer and autumn, as well as during high-concentration ozone events (with an hourly ozone value higher than 93 ppbv) throughout the year. However, in spring and winter, ozone formation was more likely to be VOC-limited for an extended period of time.

It should be noted that the results presented above are based on observational data, and the discussion of ozone formation regimes in Guangzhou is only based on a comparison with the VOC/NO_x ratios reported for Los Angeles. Further investigations using numerical simulations are needed to obtain more detailed and robust conclusions. The application of various numerical models (e.g. Observation-Based Model (OBM), Weather Research and Forecasting-Chemistry Model (WRF-Chem) and the U.S. Environmental Protection Agency's Community Multi-scale Air Quality (CMAQ)) to simulate ozone pollution in the atmosphere is imperative to fully understand the formation of ozone from VOCs and NO_x.

Acknowledgements This research work is funded by the National Natural Science Foundation of China (41175117, 40875090, 41373116), National "973" Program (2011CB403400), Natural Science Foundation of Guangdong Province (S2012010008749), National Natural Science Foundation of China and Guangdong Province Joint Fund (No. U1201232), Special Research Project of Public Service Sectors (Weather) (GYHY201306042), and Science and Technology Sponsorship Program of Guangdong Province (2010A030200012). Constructive suggestions from anonymous reviewers are great appreciated.

References

An, J., Zhu, B., Wang, H., Li, Y., Lin, X., and Yang, H.: Characteristics and source apportionment of VOCs measured in an industrial area of Nanjing, Yangtze River Delta, China, Atmos. Environ., 97, 2014

Atkinson, R. and Arey, J.: Atmospheric degradation of volatile organic compounds, Chem. Rev., 103, 4605–4638, 2003.

Atkinson, R.: Gas-phase tropospheric chemistry of organic compounds: A review, Atmos. Environ., 24A, 1-41, 1990.

Atkinson, R.: Atmospheric chemistry of VOCs and NOx, Atmos. Environ., 34, 2063–2101, 2000.

Bloomer, B. J., Stehr, J. W., Piety, C. A., Ross, J. S., and Dickerson, R. R.: Observed relationships of ozone air pollution with temperature and emissions, Geophys. Res. Lett., 36, L09803, doi:10.1029/2009GL037308, 2009.

Bloomer, B. J., Vinnikov, K. Y., and Dickerson, R. R.: Changes in seasonal and diurnal cycles of ozone and temperature in the eastern US, Atmos. Environ., 44, 1–9, 2010.

Carter, W. P. L.: Development of ozone reactivity scales for volatile organic compounds, J. Air Waste Manage., 44, 881–899, 1994.

Castellanos, P., Stehr, J. W., Dickerson R. R., and Ehrman, S. H.: The sensitivity of modeled ozone to the temporal distribution of point, area, and mobile source emissions in the eastern United States, Atmos. Environ., 43, 4603–4611, 2009.

Chameides, W. L., Fehsenfeld, F., Rodgers, M. O., Cardelino, C., Martinez, J., Parrish, D., Lonneman, W., Lawson, D R., Rasumssen, R. A., Zimmerman, P., Greenberg, J., Middleton, P. and Wang, T.: Ozone precursor relationships in the ambient atmosphere. J. Geophys. Res., 97, 6037-6055, 1992.

Chan, C. K. and Yao, X. H.: Air pollution in mega cities in China, Atmos. Environ., 42(1), 1–42, 2008.

Cheng, H. R., Guo, H., Saunders, S. M., Lam, S. H. M., Jiang, F., Wang, X. M., Simpson, I. J., Blake, D. R., Louie, P. K. K., and Wang T. J.: Assessing photochemical ozone formation in the Pearl River Delta with a photochemical trajectory model, Atmos. Environ., 44, 4199–4208, 2010.

Deng, X. J., Wang, X. M., Zhao, C. S., Ran, L., Li, F., Tan, H. B., Deng, T., Wu, D., and Zhou, X. J.: The mean concentration and chemical reactivity of VOCs of typical processes over Pearl River Delta Region, China Environ. Sci., 30, 1153 - 1161, 2010 (in Chinese).

Dunlea, E. J., et al..: Evaluation of nitrogen dioxide chemiluminescence monitors in a polluted urban environment, Atmos. Chem. Phys., 7, 2691-2704, 2007.

Darnall, K. R., Lloyd, A. C. Winer, A. M. and Pitts Jr., J. N.: Reactivity scale for atmospheric hydrocarbons based on reaction with hydroxyl radical, Environ. Sci. Technol., 10, 692–696,1976.

Dodge, M. C.：Combined effects of organic reactivity and NMHC/ NOx ratio on photochemical oxidant formation - a modeling study, Atmos. Environ., 18, 1657 - 1665, 1984.

GB 3095-2012: *Ambient air quality standards*, (Ministry, of Environmental Protection, Beijing, China, 2012), to be implemented from 2016-01-01.

Geng, F. H., Tie, X. X., Xu, J. M., Zhou, G. Q., Peng, L., Gao, W., Tang, X., and Zhao, C. S.: Characterizations of ozone, NOx, and VOCs measured in Shanghai, China, Atmos. Environ., 42, 6873–6883, 2008.

Guo, H., Jiang, F., Cheng, H. R., Simpson, I. J., Wang, X. M., Ding, A. J., Wang, T. J., Saunders, S. M., Wang, T., Lam, S. H. M., Blake, D. R., Zhang, Y. L., and Xie, M.: Concurrent observations of air pollutants at two sites in the Pearl River Delta and the implication of regional transport, Atmos. Chem. Phys., 9, 7343–7360, doi:10.5194/acp-9-7343-2009, 2009.

Kanaya, Y., Pochanart, P., Liu,Y., Li,J., Tanimoto,H., Kato,S., Suthawaree,J., Inomata,S., Taketani,F., and K. Okuzawa.: Rates and regimes of photochemical ozone production over Central East China in June 2006: A box model analysis using comprehensive measurements of ozone precursors, Atmos. Chem. Phys, 9(20), 7,711–7,723,2009.

Lawrimore, J. H., Das, M. and Aneja, V. P.: Vertical sampling and analysis of nonmethane hydrocarbons for ozone control in urban North Carolina. J. Geophys. Res., 100, 22785-22793, 1995.

Li, L., Wang, X.: Seasonal and diurnal variations of atmospheric Non-methane hydrocarbons in Guangzhou, China, Int. J. Environ. Res. Public Health, 9, 1859-1873, 2012.

Li, Y.: Numerical studies on ozone source apportionment and formation regime and their implications on control strategies, Hong Kong University of Science and Technology, Hong Kong, 2011.

Li, Y., Lau, K. H., Fung, C. H., Zheng, J. Y., and Liu, S. C.: Importance of NOx control for peak ozone reduction in the Pearl River Delta region, J. Geophys. Res., 118, 9428–9443, 2013.

Liu, Y., Shao, M., Fu, L. L., Lu, S. H., Zeng, L. M., and Tang, D. G.: Source profiles of volatile organic compounds (VOCs) measured in China: Part I, Atmos. Environ., 42, 6247–6260, 2008.

Middleton, P., Stockwell, W. R., and Carter, W. P. L.: Aggregation analysis of volatile organic compound emissions for regional modeling, Atmos. Environ., 24A, 1107–1133, 1990.

Qin, Y., Tonnesen, G.S., and Wang, Z.: One-hour and eight-hour average ozone in the California South Coast air quality management district: Trends in peak values and sensitivity to precursors, Atmos. Environ., 38, 2197-2207, 2004.

Ran, L., Zhao, C. S., Geng, F. H., Tie, X. X., Xu, T., Li, P., Guang, Q. Z., Qiong, Y., Xu, J. M., and Guenther, A.: Ozone photochemical production in urban Shanghai, China: analysis based on ground level observations, J. Geophys. Res., 114, doi:10.1029/2008JD010752, 2009.

Ran, L., Zhao, C. S., Xu, W. Y., Lu, X. Q., Han, M., Lin, W. L., Yan, P., Xu, X. B., Deng, Z. Z., Ma, N., Liu, P. F., Yu, J., Liang, W. D., and Chen, L. L.: VOC reactivity and its effect on ozone production during the HaChi summer campaign, Atmos. Chem. Phys., 11, 4657–4667, doi:10.5194/acp-11-4657-2011, 2011.

Russell, A., Milford, J., Bergin, M. S., McBride, S., McNair, L., Yang, Y., Stockwell, W. R., and Croes, B.: Urban ozone control and atmospheric reactivity of organic gases, Science, 269, 491-495, 1995.

Shao, M., Zhang, Y. H., Zeng, L. M., Tang, X. Y., Zhang, J., Zhong, L. J., and Wang, B. G.:

Ground-level ozone in the Pearl River Delta and the roles of VOC and NOx in its production, Environ. Manage., 90, 512–518, 2009.

Sillman, S.: The use of NOy, H2O2, and HNO3 as indicators for ozone-NOx-hydrocarbon sensitivity in urban locations, J. Geophys. Res., 100, 14175–14188, 1995.

Sillman, S.: The relation between ozone, NOx and hydrocarbons in urban and polluted rural environment, Atmos. Environ., 33, 1821–1845, 1999.

Sillman, S., and West.J.: Reactive nitrogen in Mexico City and its relation to ozone-precursor sensitivity: Results from photochemical models, Atmos. Chem. Phys., 9(11), 3,477–3,489, 2009.

Seinfeld, J. H.: Urban air pollution: State of the science, Science, 243,745-752, 1989.

Seinfeld, J.H.: Rethinking the ozone problem in urban and regional air pollution, Natl. Acad. Press, Washington, DC, 1991.

Stephens, S., Madronich, S., Wu, F., Olson, J.B., Ramos, R., Retama,A., and Munoz,R.: Weekly patterns of Mexico City's surface concentrations of CO, NOx, PM10 and O3 during1986-2007,Atmos.Chem.Phys., 8, 5313-5325,2008.

Tie, X., Madronich, S., Li, G. H., Ying, Z. M., Zhang, R. Y., Garcia, A. R., Taylor, J. L., and Liu, Y. B.: Characterizations of chemical oxidants in Mexico City: A regional chemical/ dynamical model (WRF-Chem) study, Atmos. Environ., 41, 1989–2008, 2007.

Trainer, M.: Correlation of ozone with NOy in photochemically aged air, J. Geophys. Res., 98, 2917-2925, 1993.

Wang, B. G., Zhang, Y. H., and Shao, M.: Special and temporal distribution character of VOCs in the ambient air of Pearl River Delta region, Environ. Sci., 25, 7–15, 2004 (in Chinese).

Wang, T., Wei, X. L., Ding, A. J., Poon, C. N., Lam, K. S., Li, Y. S., Chan, L. Y., and Anson, M.: Increasing surface ozone concentrations in the background atmosphere of Southern China, 1994–2007, Atmos. Chem. Phys., 9, 6217–6227, doi:10.5194/acp-9-6217-2009, 2009.

Wang, T. J., Jiang, F., Deng, J. J., Shen, Y., Fu, Q. Y., Wang, Q., Fu, Y., Xu, J. H., and Zhang, D. N.: Urban air quality and regional haze weather forecast for Yangtze River Delta region, Atmos. Environ., 58, 70–83, 2012.

Wang, X. M., Carmichael, G., Chen, D. L., Tang, Y. H., and Wang, T. J.: Impacts of different emission sources on air quality during March 2001 in the Pearl River Delta (PRD) region, Atmos. Environ., 39, 5227–5241, 2005.

Zhang, R. Y., Lei, W. F., Tie, X. X., and Hess, P.: Industrial emissions cause extreme diurnal urban ozone variability, Proc. Natl. Acad. Sci. USA, 101, 6346–6350, 2004.

Zhang, Y. H., Su, H., Zhong, L. J., Cheng, Y. F., Zeng, L. M., Wang, X. S., Xiang, Y. R., Wang, J. L., Gao, D. F., and Shao, M.: Regional ozone pollution and observation-based approach for analyzing ozone–precursor relationship during the PRIDE-PRD2004 campaign, Atmos. Environ., 42, 6203–6218, doi:10.1016/j.atmosenv.2008.05.002, 2008.

Zhao, P. S., Zhang, X. L., Xu, X. F., and Zhao X. J.: Long-term visibility trends and characteristics in the region of Bejing, Tianjin, and Hebei, China, Atmos. Res., 101, 711–718, 2011.

Zou, Y., Deng, X. J., Wang, B. G., Li, F., and Huang, Q.: Pollution characteristics of volatile organic compounds in Panyu Composition Station, Environ. Sci., 33, 808–813, 2013 (in

Chinese).

Table 1. The wind speed and temperature in each season (from June 2011 to May 2012) at GPACS.

		Minimum	**Maximum**	**Mean**	**Median**
Spring	Wind speed/m.s^{-1}	0.0	5.4	1.3	1.2
	Temperature/℃	9.4	35.5	22.6	22.9
Summer	Wind speed/m.s^{-1}	0.0	6.0	1.4	1.2
	Temperature/℃	23.9	37.1	29.4	28.8
Autumn	Wind speed/m.s^{-1}	0.0	5.7	1.5	1.4
	Temperature/℃	16.2	35.3	25.2	25.2
Winter	Wind speed/m.s^{-1}	0.0	6.3	1.5	1.4
	Temperature/℃	4.7	26.9	14.2	14.1

Table 2. The calibration curves and detection limits of VOC species

Target Compound	Calibration Curve	Correlation Coefficient	Detection Limit (ppbv)
Ethene	y=1.0188x+0.2659	0.997	0.07
Acetylene	y=1.0409x+0.1756	0.998	0.08
Ethane	y=1.0162x+0.2891	0.997	0.08
Propene	y=0.9959x+0.1506	0.999	0.07
Propane	y=0.9824x+0.2082	0.998	0.09
i-Butane	y=0.9753x+0.3785	0.994	0.05
1-Butene	y=0.9587x+0.3641	0.994	0.06
n-Butane	y=0.9776x+0.3718	0.994	0.05
trans-2-Butene	y=0.9746x+0.2747	0.997	0.05
cis-2-Butene	y = 0.9834x+0.1606	0.999	0.06
i-Pentane	y=0.9753x+0.2135	0.998	0.07
1-Pentene	y = 0.919x+0.1626	0.998	0.05
n-Pentane	y = 0.9557x+0.2038	0.984	0.07
Isoprene	y=1.0304x+0.1653	0.998	0.07
trans-2-pentene	y=0.9753x+0.2135	0.998	0.07
cis-2-pentene	y = 0.9557x+0.2038	0.984	0.07
2,2-Dimethylbutane	y=0.9731x+0.1971	0.998	0.07
Cyclopentane	y=0.9993x+0.1412	0.997	0.06
2,3-Dimethylbutane	y = 0.919x+0.1626	0.999	0.07
2-Methylpentane	y = 0.9557x+0.2038	0.984	0.07
3-Methylpentane	y=0.9753x+0.2135	0.998	0.07
1-Hexene	y=0.9700x+0.3300	0.995	0.05
n-Hexane	y=0.9915x+0.2626	0.997	0.06
Methylcyclopentane	y = 0.9749x+0.1832	0.999	0.07
2,4-Dimethylpentane	y=0.9993x+0.1412	0.999	0.05
Benzene	y=0.9753x+0.2835	0.997	0.06
Cyclohexane	y=0.9841x+0.2744	0.997	0.07
2-methylhexane	y=0.9744x+0.2979	0.996	0.05
2,3-dimethylpentane	y=0.9779x+0.2953	0.997	0.05
3-methylhexane	y=0.9735x+0.3374	0.995	0.05
2,2,4-trimethylpentane	y=0.9696x+0.3947	0.994	0.05
n-Heptane	y=0.9678x+0.3635	0.994	0.05
Methylcyclohexane	y=0.9819x+0.3629	0.995	0.05
2,3,4-trimethylpentane	y=0.9691x+0.3994	0.994	0.04
Toluene	y=0.9696x+0.3397	0.995	0.05
2-methylheptane	y=0.9603x+0.4835	0.990	0.04
3-methylheptane	y=0.9625x+0.4550	0.991	0.04
n-Octane	y=0.9524x+0.5082	0.989	0.04
Ethylbenzene	y=0.9629x+0.4253	0.992	0.04
m, p- Xylenes	y=0.9541x+0.5844	0.986	0.03
Styrene	y=0.9524x+0.4132	0.991	0.04

o-Xylene	y=0.9515x+0.4926	0.989	0.04
n-Nonane	y = 0.9878x+0.1635	0.998	0.04
i-Propylbenzene	y=0.9418x+0.5162	0.986	0.04
n-Propylbenzene	y=0.9426x+0.5468	0.986	0.04
m-Ethyltoluene	y = 0.9532x+0.4838	0.989	0.04
p-Ethyltoluene	y = 0.9554x+0.3953	0.992	0.04
1,3,5-Trimethylbenzene	y = 0.951x+0.4724	0.989	0.04
o-Ethyltoluene	y = 0.9784x+0.0956	0.999	0.04
1,2,4-trimethylbenzene	y = 0.9563x+0.4509	0.991	0.03
n-Decane	y = 0.9651x+0.3068	0.995	0.04
1,2,3-trimethylbenzene	y = 0.9537x+0.3191	0.993	0.04
m-Diethylbenzene	y = 0.9541x+0.4494	0.991	0.04
p-Diethylbenzene	y = 0.9607x+0.3788	0.993	0.04
n-Undecane	y = 0.9519x+0.3329	0.992	0.04
n-Dodecane	y=0.9890x+0.2711	0.993	0.05

Table 3. Daily average of VOCs categories, NO_x and ozone in each season (from June 2011 to May 2012）at GPACS

		Alkanes /ppbv	**Alkenes /ppbv**	**Aromatics/ppbv**	**VOCs /ppbv**	**NOx /ppbv**	**O_3 /ppbv**
Spring	March	20.84	5.26	8.50	34.60	76.39	12.46
	April	25.11	5.86	11.33	42.30	35.17	16.02
	May	21.45	5.47	10.94	37.86	25.29	24.55
Summer	June	19.74	6.62	14.23	40.60	24.40	24.26
	July	20.07	6.72	12.90	39.69	24.70	24.26
	August	22.36	9.12	9.99	41.46	21.75	28.26
Autumn	September	20.82	7.80	8.95	37.57	25.18	29.67
	October	22.26	5.63	8.89	36.78	26.59	25.34
	November	39.16	10.24	14.16	63.57	39.98	21.78
Winter	December	33.61	8.47	5.97	48.05	39.14	20.37
	January	32.13	7.96	7.54	47.63	34.82	9.31
	February	-	-	-	-	52.69	9.97

Table 4. Properties of VOCs at GPACS from June 2011 to May 2012.

Compound	MIR[a]	$K^{b}_{OH} \times HR^{12}$	Mixing ratio （ppbv）	Mixing ratio （ppbC）
Alkanes				
Ethane	0.25	0.27	3.66	7.31
Propane	0.46	1.15	4.34	13.02
i-Butane	1.18	2.34	2.67	10.68
n-Butane	1.08	2.54	3.07	12.28
Cyclopentane	2.24	5.16	0.15	0.77
i-Pentane	1.36	3.90	1.72	8.61
n-Pentane	1.22	3.94	1.37	6.86
Methylcyclopentane	1.46	5.10	0.32	1.94
2,3-Dimethylbutane	1.07	6.30	0.13	0.76
2,2-Dimethybutane	0.82	2.32	0.37	2.22
2-Methylpentane	1.40	5.60	0.88	5.29
3-Methylpentane	1.69	5.70	0.75	4.51
n-Hexane	1.14	5.60	1.43	8.56
2,4-Dimethylpentane	1.11	5.70	0.37	0.41
Cyclohexane	1.14	7.49	1.65	9.90
2-Methylhexane	1.09	6.90	0.58	4.04
2,3-Dimethylpentane	1.25	5.10	0.26	1.82
3-Methylhexane	1.50	5.10	0.52	3.66
2,2,4-Trimethylpentane	1.20	3.68	0.22	1.79
n-Heptane	0.97	7.15	0.32	2.24
Methylcyclohexane	1.56	10.4	0.26	1.81
2,3,4-Trimethylpentane	0.97	7.00	0.12	0.96
2-Methylheptane	1.12	8.30	0.08	0.66
3-Methylheptane	0.80	8.60	0.08	0.68
n-Octane	0.68	8.68	0.19	1.54
n-Nonane	0.59	10.20	0.35	3.18
n-Decane	0.52	11.60	0.03	0.29
n-Undecane	0.47	13.20	0.17	1.92
n-Dodecane	0.38	14.20	0.14	1.65
Alkenes				
Ethene	7.40	8.50	2.99	5.97
Propene	11.57	26.3	1.32	3.96
trans-2-Butene	15.20	64.0	0.28	1.14
1-Butene	9.57	31.4	0.44	1.77
cis-2-Butene	14.26	56.4	0.22	0.86
trans-2-Pentene	10.47	67.0	0.03	0.15
1-Pentene	7.07	31.4	0.05	0.23
cis-2-Pentene	10.28	65.0	0.19	0.97
Isoprene	10.48	101	1.14	5.72
1-Hexene	—	—	0.67	3.99

Aromatics				
Benzene	0.42	1.23	0.62	3.72
Toluene	3.93	5.96	4.59	32.10
Ethylbenzene	2.96	6.96	1.48	11.81
m,p-Xylene	8.54	20.5	1.41	11.24
Styrene	1.66	58.0	0.41	3.25
o-Xylene	7.58	13.6	0.66	5.28
i-Propylbenzene	2.45	6.60	0.10	0.86
n-Propylbenzene	1.96	5.70	0.23	2.05
m-Ethyltoluene	7.39	18.6	0.25	2.22
p-Ethyltoluene	4.39	11.8	0.21	1.89
1,3,5-Trimethylbenzene	11.75	56.7	0.21	1.86
o-Ethyltoluene	5.54	11.9	0.27	2.47
1,2,4-Trimethylbenzene	8.83	32.5	0.21	1.92
1,2,3-Trimethylbenzene	11.94	32.7	0.15	1.32
m-Diethylbenzene	7.08	15.0	0.12	1.25
p-Diethylbenzen	4.39	10.0	0.11	1.05

MIR[a] denotes maximum incremental reactivity (Carter, et al., 1994).

k^{b}_{OH} denotes rate constant of VOCs react with hydroxyl radicals at 298K (Atkinson and Arey,2003).

Table 5. Relative contributions to ozone formation by the top 10 VOCs species based on the Propy-Equiv and the MIR scales from June 2011 to May 2012 at GPACS.

OH Reactivity Rank		MIR Rank	
Compound	Percentage（%）	Compound	Percentage（%）
Isoprene	19.97	Toluene	16.26
m,p-Xylene	7.97	m,p-Xylene	12.48
Toluene	6.62	Isoprene	7.99
Styrene	6.51	Propene	6.30
1,3,5-Trimethylbenzene	3.82	Ethene	6.07
Propene	3.60	o-Xylene	5.21
Ethylbenzene	2.85	Ethylbenzene	4.54
Cyclohexane	2.56	1,3,5-Trimethylbenzene	2.87
trans-2-Butene	2.51	trans-2-Butene	2.37
o-Xylene	2.48	1,2,4-Trimethylbenzene	2.22

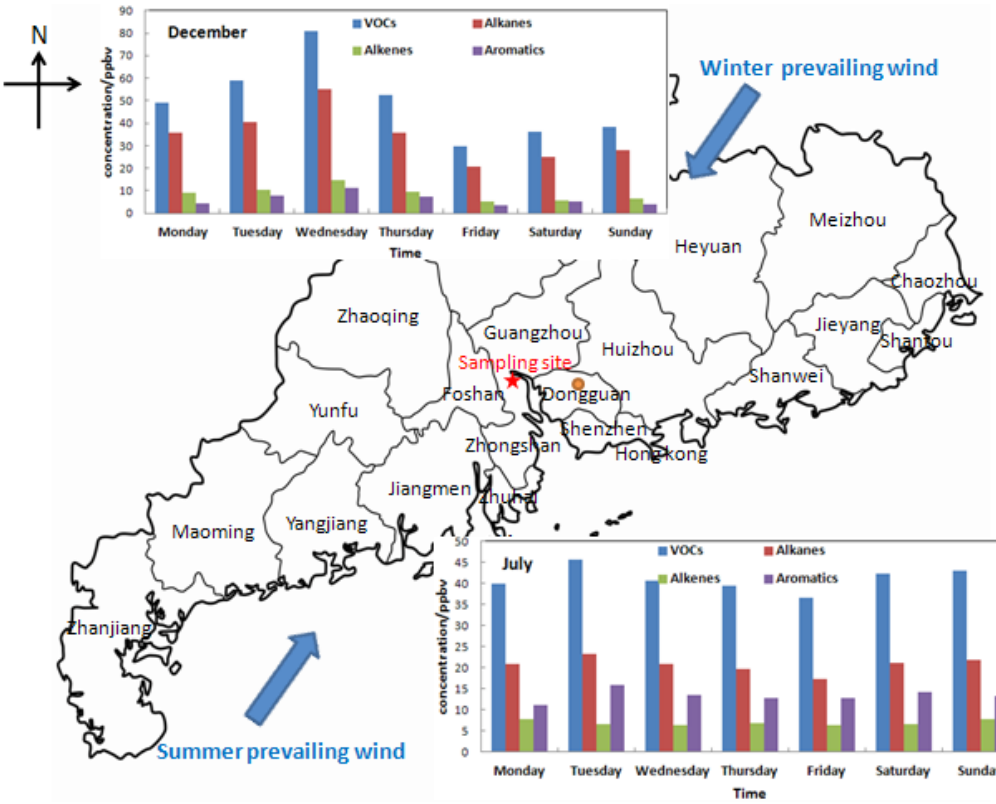

Fig. 1. The location of observation site at GPACS and its surrounding area, the pentagram represents the sampling site, and the circle represents the Dongguan City. The VOCs profiles in July when the summer prevailing wind is SW and in December when the winter prevailing wind is NE are shown in the map.

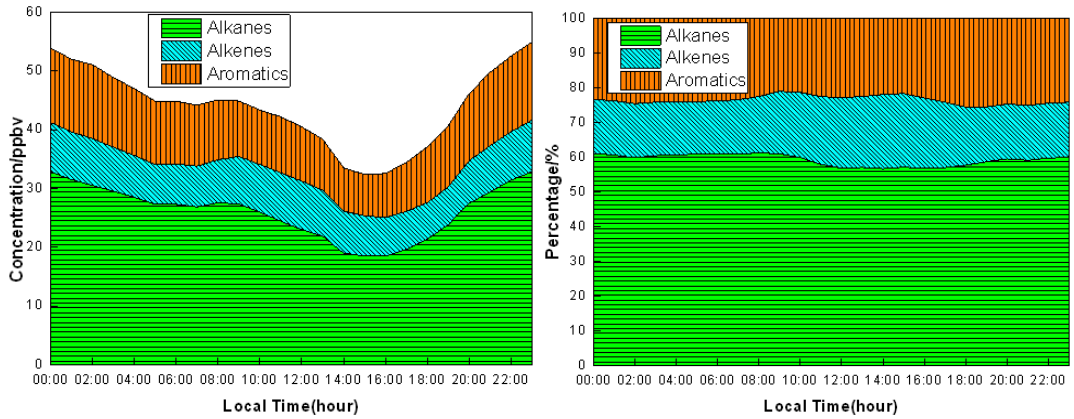

Fig. 2. Diurnal variation of hourly averaged concentrations of three categories of VOCs in ppbv and in fraction (from June 2011 to May 2012) at GPACS

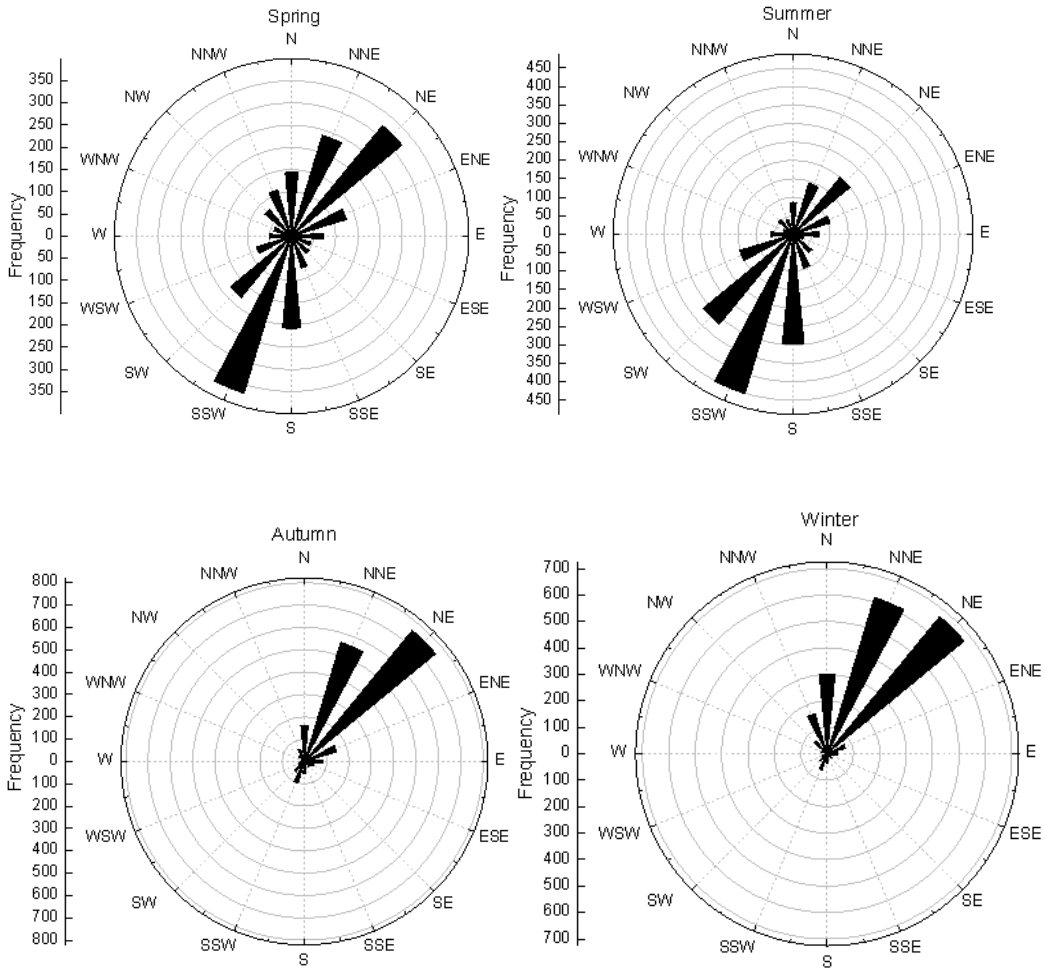

Fig. 3. Wind rose diagrams for the frequencies of wind direction in each season from June 2011 to May 2012 at GPACS.

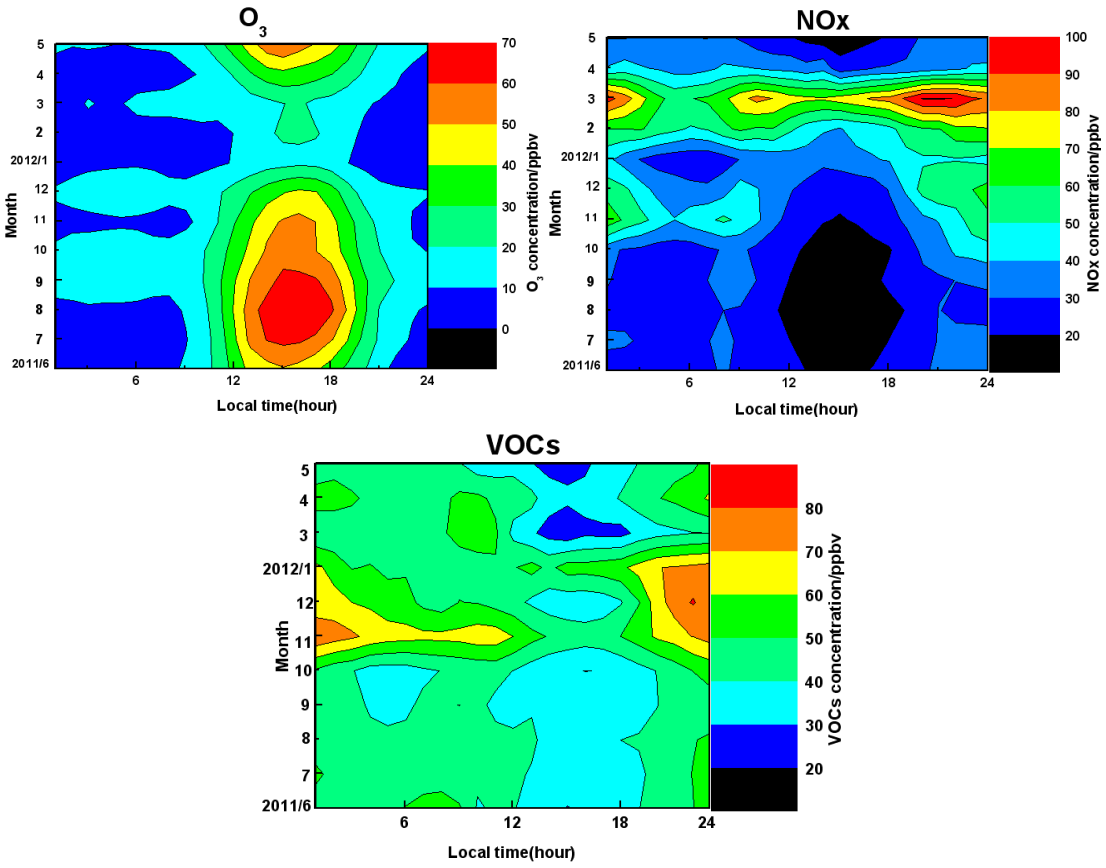

Fig. 4. The seasonal-diurnal variations with daily 1-hour averages of ozone, NO_x and VOCs from June 2011 to May 2012 at GPACS.

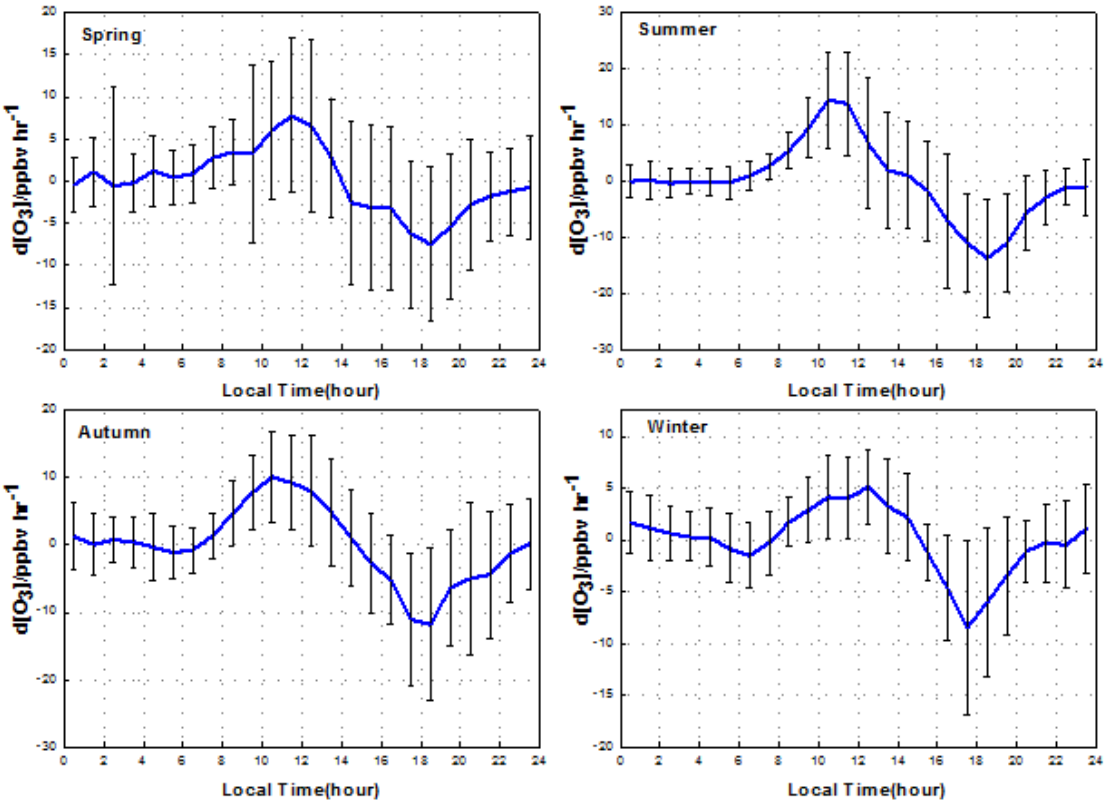

Fig. 5. Average diurnal trends in ozone for each season during June 2011 to May 2012 at GPACS. The blue lines represent hourly mean values and the black bars represent the standard deviation.

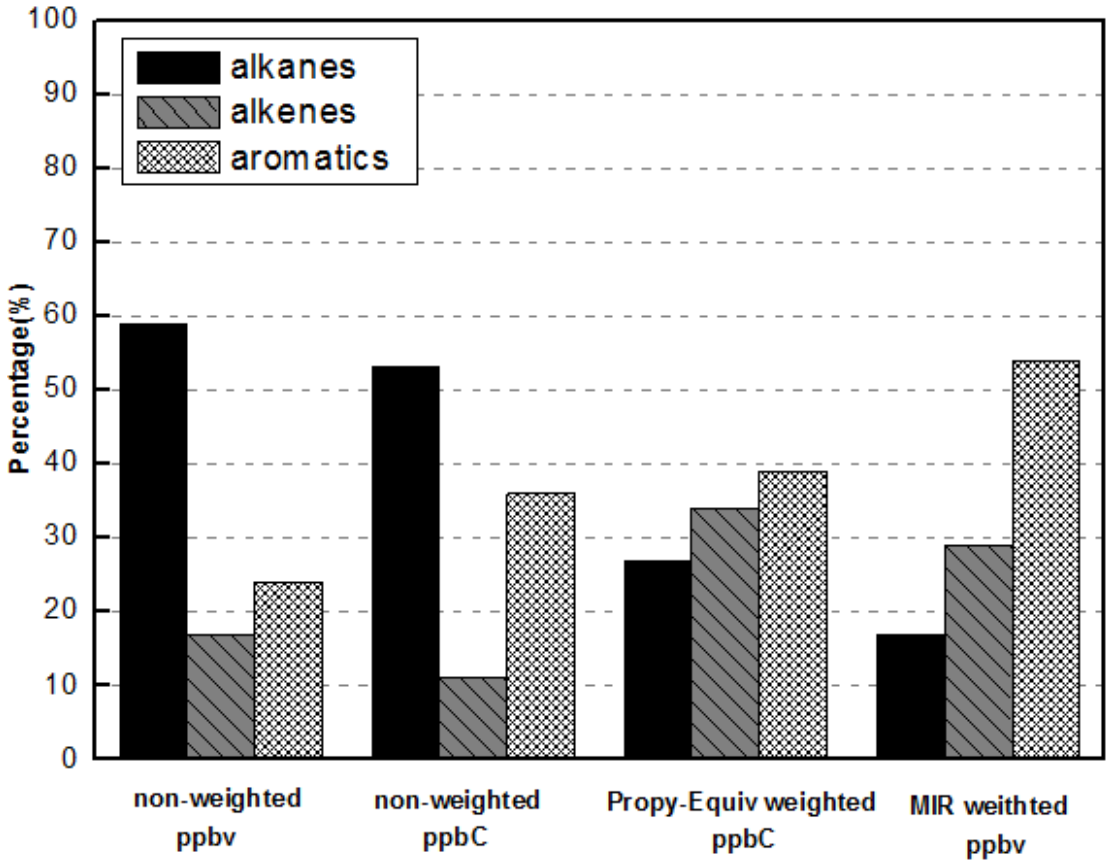

Fig. 6. VOC profiles based on different scales from June 2011 to May 2012 at GPACS.

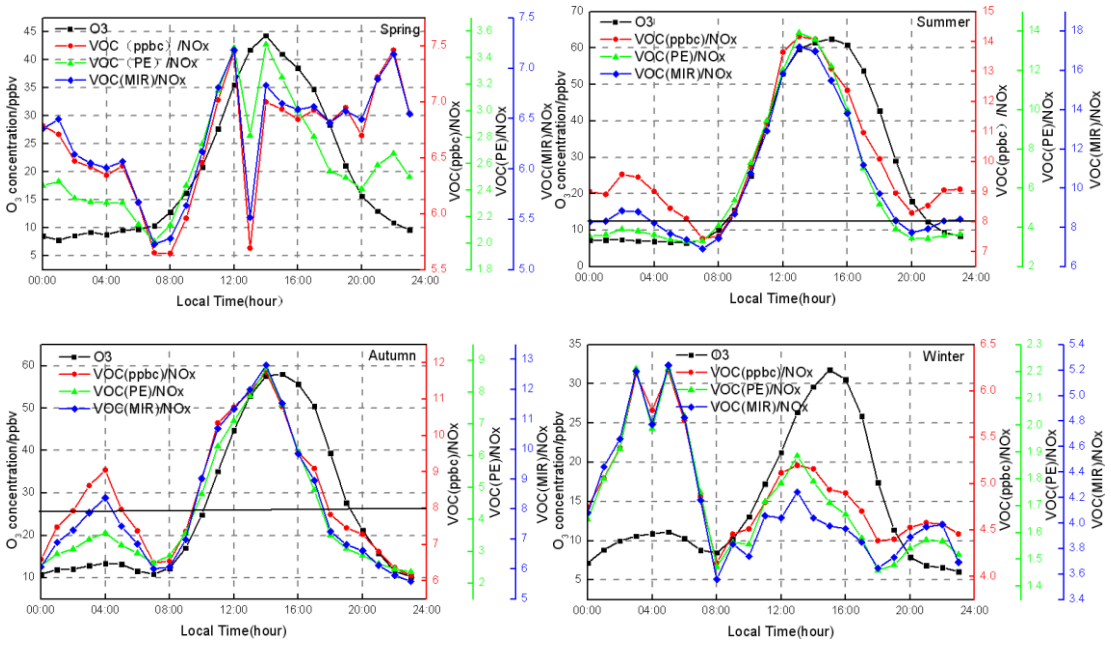

Fig. 7. The diurnal patterns of VOC/NOx ratios calculated by three different ways, as well as ozone concentrations, for each season from summer 2011 to spring 2012 at GPACS. Black level lines represent the VOC(ppbC)/NOx ratio of 8:1.

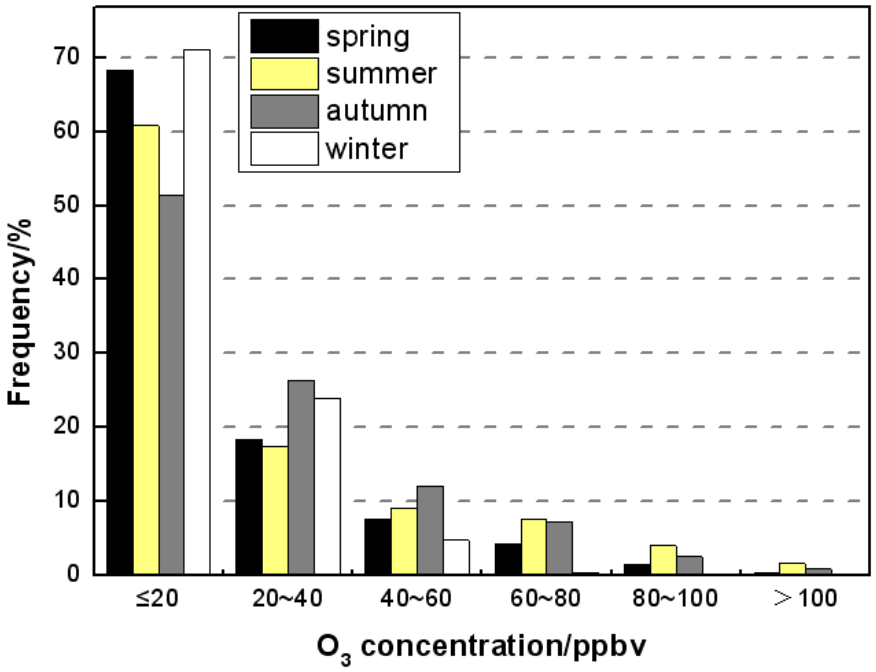

Fig. 8. The seasonal frequency distribution of hourly ozone concentration from summer 2011 to spring 2012 at GPACS, the frequency of hourly ozone concentration in each corresponding season is plotted by bar.

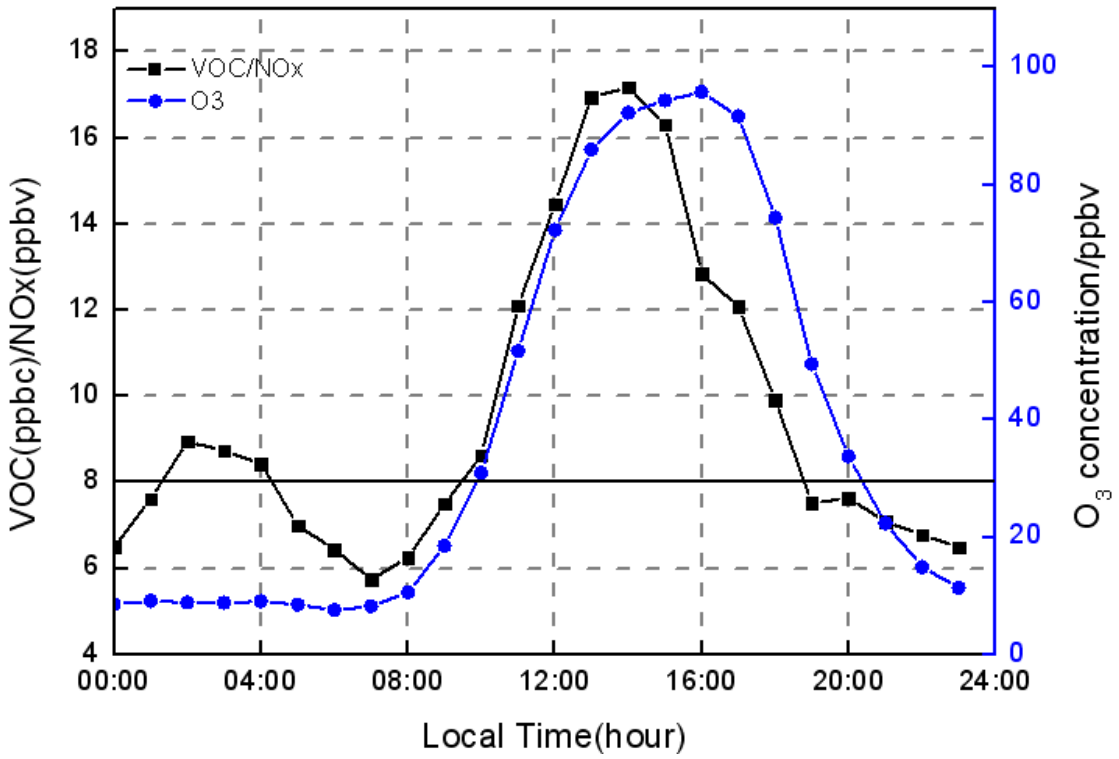

Fig. 9. The variation patterns of VOC/NOx ratio and ozone concentration at high ozone episode at GPACS. High ozone episode refers to the day with an hourly ozone value higher than 93 ppbv. A black level line represents the VOC/NO_x of 8:1.